

**ISTANBUL TECHNICAL UNIVERSITY ★ INSTITUTE OF SCIENCE AND
TECHNOLOGY**

**A STUDY ON KINEMATIC MANIPULABILITY MEASURES FOR
REDUNDANT ARMS: ELLIPSOIDS AND POLYTOPES**

MSC THESIS

**Elec. Eng. Aykut KILIÇ
(518021016)**

Date of submission : 9 May 2005

Date of defence examination : 23 May 2005

Supervisor (Chairman) : Assoc. Prof. Dr. Hakan Temeltaş

Members of the Examining Committee : Prof.Dr. Serhat Şeker (İ.T.Ü.)

Assoc. Prof. Dr. Ata Muğan (İ.T.Ü.)

May 2005

Preface

I would like to thank to my supervisor Asc. Prof. Hakan Temeltaş for his great help and patience. Without his valuable effort, this study would not be possible. I'd also like to thank to my family for the confidence they supported. Additionally, special thanks to Murat Yeşiloğlu, Bülent Ünver, Ergün Güraslan and Ömer Rüştü Ergen for their help.

Aykut KILIÇ

May 2005

Table of Contents

| | <u>Page No</u> |
|---|----------------|
| Preface..... | i |
| Abbreviations | iii |
| Nomenclature | v |
| 1. Introduction | 1 |
| 2. Control of Redundant Manipulators..... | 2 |
| 2.1. Task Decomposition..... | 2 |
| 3. Kinematic Manipulability Measures | 6 |
| 3.1. Manipulability Ellipsoid | 6 |
| 3.1.1. Singular Value Decomposition | 7 |
| 3.1.2. Diagonalization of a matrix..... | 12 |
| 3.1.3. Pseudo-inverse. | 13 |
| 3.1.4. Formulating the Null-Space of a Matrix | 14 |
| 3.1.5. Generalized Solution | 15 |
| 3.2. Manipulability Polytope..... | 16 |
| 3.2.1. Computation of vertices: | 16 |
| 3.2.2. Derivation of a Manipulability Index Based on Polytope..... | 17 |
| 4. Simulation Results | 19 |
| 4.1. Computation of manipulator Jacobian | 19 |
| 4.2. Results from manipulability ellipsoids and manipulability polytopes with comparative results..... | 21 |
| 5. Conclusion | 25 |
| References | 26 |
| Appendix A. UML Diagrams of the communications library | 27 |

Abbreviations

| | |
|--------|-------------------------------|
| EVD: | Eigen-value decomposition. |
| SVD: | Singular value decomposition. |
| MPA10: | Mitsubishi PA10 Robot arm. |
| P560: | Puma 560 Robot Arm. |

List of Figures

| | <u>Page No</u> |
|--|----------------|
| Figure 2.1: Composing a task by merging subtasks..... | 3 |
| Figure 3.1: Manipulability ellipsoid of an arbitrary manipulator..... | 7 |
| Figure 3.2: Geometrical representation of the singular value decomposition. \mathbf{U} and \mathbf{V} are rotations and reflections, $\mathbf{\Sigma}$ is a stretching matrix..... | 8 |
| Figure 3.3: Projection of a vector onto a subspace | 14 |
| Figure 3.4: Construction of manipulability polytopes in 2-dimensional task space for a 3 joint robot. (a) Polytope made of two vectors. (b) Polytope after adding one more vector. | 17 |
| Figure 3.5: Examples of Cone-cell in (a) 2-dimensional task space and (b) 3 dimensional task space and non-Con-cell in (c) 2-dimensional task space and (d) 3 dimensional task-space..... | 18 |
| Figure 4.1: Geometric layout of links and \mathbf{h} vectors. | 19 |
| Figure 4.2: Manipulability polytope of a two link planar arm..... | 21 |
| Figure 4.3: Manipulability ellipsoid and polytope of a two link planar arm for the same configuration | 22 |
| Figure 4.4: Manipulability ellipsoid and polytope of a MPA10 for the same joint configuration. | 23 |
| Figure 4.5: Manipulability ellipsoid and polytope of a P560 for the same configuration. | 24 |
| Figure A.1: Class diagram for the irlroot..... | 27 |
| Figure A.2: Sequence diagram for protocol driver abstraction..... | 28 |
| Figure A.3: Class diagram for ARCNET communication driver. | 28 |
| Figure A.4: ARCNET state diagram for MPA10. | 29 |
| Figure A.5: Class diagram for concrete ARCNET protocol and message classes. .. | 29 |

Nomenclature

| | |
|----------------------------------|---|
| \mathbf{q} | Manipulator configuraion vector. (Joint positions) |
| $\mathbf{J}(\mathbf{q})$ | Manipulator Jacobian matrix. |
| $\ \mathbf{q}\ $ | l_2 -norm (euclidian norm) of vector \mathbf{q} . |
| \mathbf{U} | A unitary matrix. |
| \mathbf{D} | A diagonal matrix. |
| \mathbf{T} | A triangular matrix. |
| \mathbf{A}^* | Complex-conjugate transpose (hermitian) of matrix \mathbf{A} . |
| \mathbf{A}^+ | Generalized Moore-Penrose inverse (pseudo-inverse) of matrix \mathbf{A} . |
| \mathbf{A}^T | Transpose of matrix \mathbf{A} . |
| $\mathbf{U}, \Sigma, \mathbf{V}$ | Orthogonal, diagonal, orthogonal matrices for SVD. |
| m | Row count of the related matrix. |
| n | Column count of the related matrix. |
| λ_i | i -th eigenvalue of the related matrix. |
| σ_i | i -th singular value of the related matrix. |
| \mathbf{v}_j | j -th vertex of a polytope. |
| \mathbf{u}_i | i -th column vector for matrix \mathbf{U} . |
| \mathbf{S} | Eigen-vector matrix of EVD. |
| Λ | Eigen-value matrix of EVD. |
| \mathbf{P} | Projection matrix. |
| $R(\mathbf{A})$ | Range of matrix \mathbf{A} . |
| $\boldsymbol{\omega}_i$ | Angular velocity vector of origin of i -th joint. |
| \mathbf{v}_i | Linear velocity vector of origin of i -th joint. |
| \mathbf{V}_i | Spatial velocity vector of origin of i -th joint. |
| $\mathbf{l}_{j-1,j}$ | link vector for manipulator link between joints $j-1$ and j . |

FAZLALIK EKSENLI ROBOT KOLLARDA HAREKETLİLİK ÖLÇÜTLERİ: ELİPSOİD VE POLİTOP

ÖZET

Bu çalışmada hareketlilik elipsoidi, SVD, genel matris tersi ve hareketlilik politopu yöntemleri matematiksel açıdan detaylı olarak incelenmiştir. Fazlalık eksenli robotlarda iş ayrıştırma metodu işlenmiş ve her iki hareketlilik yöntemi kullanılarak fazlalık eksenli ve normal robot kollar için görsel ve sayısal sonuçlar elde edilmiş ve kıyaslanmıştır.

A STUDY ON KINEMATIC MANIPULABILITY MEASURES FOR REDUNDANT ARMS: ELLIPSOIDS AND POLYTOPES

ABSTRACT

This text describes the theory behind manipulability ellipsoids, singular value decomposition, pseudo-inverse and manipulability polytopes in mathematical aspect. Examines task decomposition approach for redundant control and compares results obtained from both manipulability measures on three types of robots covering ordinary and redundant manipulators.

1. Introduction

Manipulability ellipsoids, introduced by Yoshigawa [1], has been used to analyze manipulator dexterity by many researchers, while manipulability polytopes input a more applicable joint space constraint and results a wider solution set when compared to ellipsoids.

This text describes both methods in mathematical aspect. Singular value decomposition method used in computation of ellipsoid geometry is covered with its proof, geometrical interpretation and relation with eigen-value decomposition.

Both methods are applied on a real world case and a comparative examination of results for both are included as a conclusion.

First chapter covers task decomposition approach for the control of redundant manipulators and describes two types of solution for the additional tasks to perform when redundancy exists for initial joint configuration.

Second chapter focuses on how to evaluate manipulability for any type of manipulator and describes two major methods, manipulability ellipsoid and manipulability polytope.

Third chapter describes the forward kinematics computations for robots and applies the manipulability measure for a two link planar and, a Puma-560 type robot and to a Mitsubishi PA10 manipulator.

Finally, as a conclusion the numerical results from both approaches are compared.

2. Control of Redundant Manipulators.

If the degree of freedom of a manipulator is higher than the count necessary for the task it will perform, then it's possible to simultaneously override the target task with additional jobs and the manipulator is said to have redundancy.

Redundancy lets more complicated tasks to be performed such as obstacle avoidance, reaching behind objects, tracing trajectories require penetration with limited deviations in grip orientation which might not be possible without it. Additionally it enhances manipulator's workspace by widening mechanical limitations and assists in improving the balance in distribution of load on individual joints.

Though the additional possibilities that redundancy supply, it's optimal to select a non-redundant manipulator unless its advantages are utilized. This is because redundancy is expensive in computation, mechanical complexity, weight and cost when compared to non-redundant manipulation.

2.1. Task Decomposition

An approach to utilize capabilities supported by redundant axii of the manipulator is decomposing a task into subtasks with different priorities and perform the less prior subtask only if degree of freedom is left. For example controlling the tip position and tip orientation, avoiding from obstacles can be different subtasks. Tip position and obstacle avoidance subtasks might be critical and so with high priority, while orientation control is less important and with a lower priority, so orientation control will be implemented only if degree of freedom remains after position and obstacle avoidance control. It's also possible to have priorities dynamic as importance of subtasks might vary.

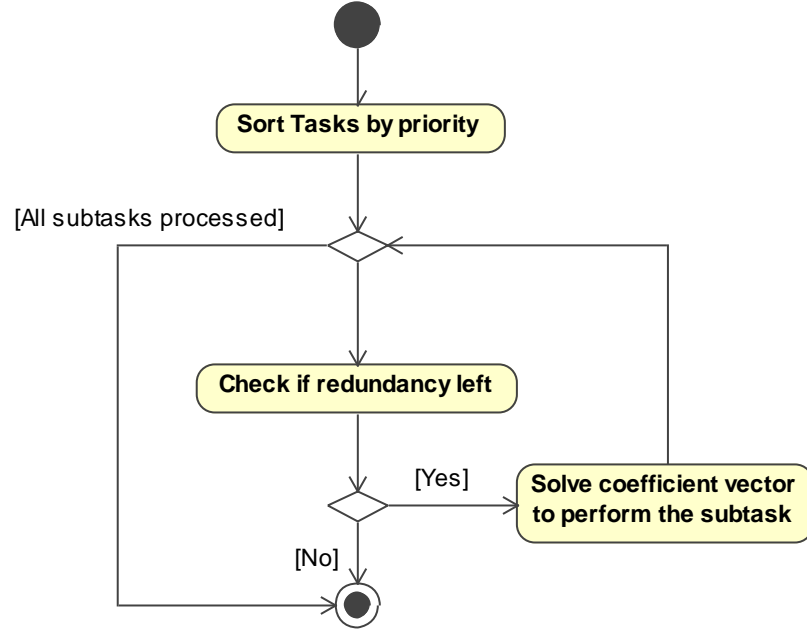


Figure 2.1: Composing a task by merging subtasks

We will formulate subtasks in two forms. In first form, subtasks defines a desired trajectory. In second form, subtask defines a criterion function which we desire to maximize. Latter is used when the desired trajectory is unknown while its evaluation is definable; for example joint limit and singularity avoidance. For the sake of simplicity, in this text we will limit the explanation by a task with two subtasks, whose prior subtask is in first form.

Let $\mathbf{q} = [q_1, \mathbf{K}, q_n]^T$ denote the configuration of a manipulator with n degrees of freedom, m_1 -dimensional vector $\mathbf{y}_1 = \mathbf{f}_1(\mathbf{q})$ to describe the first subtask and $\mathbf{y}_{1d}(t)$ to describe the desired trajectory. By definition, a vector which is suitable for describing a manipulation task is called a manipulation vector.

Differentiating first subtask gives

$$\dot{\mathbf{y}}_1 = \mathbf{J}_1(\mathbf{q})\dot{\mathbf{q}} \quad (0.1)$$

where \mathbf{J}_1 is the Jacobian matrix of \mathbf{y}_1 with respect to \mathbf{q} . For the desired trajectory of the first subtask the general solution of $\dot{\mathbf{q}}$ is

$$\dot{\mathbf{q}} = \mathbf{J}_1^+ \dot{\mathbf{y}}_{1d} + (\mathbf{I} - \mathbf{J}_1^+ \mathbf{J}_1) \mathbf{k}_1 \quad (0.2)$$

where \mathbf{k}_1 is an arbitrary n -dimensional vector. Formulation of the null-space of a matrix is described in section 3.1.4 and the general solution for a set of simultaneous equations is described in section 3.1.5.

The first term of the right hand side of the equation gives the joint velocities to perform the desired trajectory. If multiple solutions for $\dot{\mathbf{q}}$ exist this term gives the solution with the minimum euclidian norm. If no solution exists, this term minimizes $\|\mathbf{y}_{1d} - \mathbf{J}_1 \dot{\mathbf{q}}\|$ which can be counted as the best approximation to the desired trajectory. The second term gives the redundancy left after performing the first subtask.

For first case we examine a second task given by desired trajectory \mathbf{y}_{2d} . We will solve \mathbf{k}_1 so that (0.2) realizes \mathbf{y}_{2d} with minimum euclidian norm of error.

$$\dot{\mathbf{x}}_2 = \mathbf{J}_2 \dot{\mathbf{q}} \quad (0.3)$$

If we rearrange (0.2) and (0.3) in form $\dot{\mathbf{x}}_2 = \mathbf{B} \mathbf{k}_1$ to obtain the general solution of \mathbf{k}_1

$$\mathbf{y}_{2d} - \mathbf{J}_2 \mathbf{J}_1^+ \mathbf{y}_{1d} = \mathbf{J}_2 (\mathbf{I} - \mathbf{J}_1^+ \mathbf{J}_1) \mathbf{k}_1 \quad (0.4)$$

Let $\bar{\mathbf{J}}_2 = \mathbf{J}_2 (\mathbf{I} - \mathbf{J}_1^+ \mathbf{J}_1)$ for simplicity, then the general solution of \mathbf{k}_1 is

$$\mathbf{k}_1 = \bar{\mathbf{J}}_2^+ (\dot{\mathbf{x}}_{2d} - \mathbf{J}_2 \mathbf{J}_1^+ \dot{\mathbf{x}}_{1d}) + (\mathbf{I} - \bar{\mathbf{J}}_2^+ \bar{\mathbf{J}}_2) \mathbf{k}_2 \quad (0.5)$$

$(\mathbf{I} - \mathbf{J}_1^+ \mathbf{J}_1)$ is symmetric and idempotent so $(\mathbf{I} - \mathbf{J}_1^+ \mathbf{J}_1) \bar{\mathbf{J}}_2 = \bar{\mathbf{J}}_2$ holds. The desired joint velocity is

$$\dot{\mathbf{q}}_d = \mathbf{J}_1^+ \dot{\mathbf{x}}_{1d} + \bar{\mathbf{J}}_2^+ (\dot{\mathbf{x}}_{2d} - \mathbf{J}_2 \mathbf{J}_1^+ \dot{\mathbf{x}}_{1d}) + (\mathbf{I} - \mathbf{J}_1^+ \mathbf{J}_1 - \bar{\mathbf{J}}_2^+ \bar{\mathbf{J}}_2) \mathbf{k}_2 \quad (0.6)$$

If the factor of \mathbf{k}_2 is non-zero then there's still some redundancy left and we can solve \mathbf{k}_2 so that $\dot{\mathbf{q}}_d$ performs additional tasks.

If second subtask is formulated in second form, then we will solve the coefficients to maximize the criterion function. [7] is an approach for determination of \mathbf{k}_1 .

$$\mathbf{k}_1 = \xi \mathbf{k}_p \quad (0.7)$$

Where k_p is a positive constant and $\xi = [\xi_1, \dots, \xi_n]$ and,

$$\xi_i = \frac{\partial V(\mathbf{q})}{\partial \mathbf{q}_i} \quad (0.8)$$

The desired joint velocity, $\dot{\mathbf{q}}_d$ is given by,

$$\dot{\mathbf{q}}_d = \mathbf{J}_1^+ \dot{\mathbf{x}}_d + (\mathbf{I} - \mathbf{J}_1^+ \mathbf{J}_1) \xi k_p \quad (0.9)$$

Hence

$$\ddot{\mathbf{q}} = \xi^T \mathbf{J}_1 \ddot{\mathbf{x}}_d + \mathbf{x}^T (\mathbf{I} - \mathbf{J}_1^+ \mathbf{J}_1) \xi k_p \quad (0.10)$$

The second term on the right hand side is always non-negative since $(\mathbf{I} - \mathbf{J}_1^+ \mathbf{J}_1)$ is non-negative definite, causing the value of p to increase quickly under the condition that $\dot{\mathbf{q}}_d$ doesn't become excessively large. [1,7]

3. Kinematic Manipulability Measures

3.1. Manipulability Ellipsoid

Manipulability ellipsoid is an approach to quantitatively evaluate the ease of arbitrarily changing the position and orientation of the end effector of the tip of the manipulator. If joint velocities are applied with the constraint to have an euclidian norm less than 1 then the transformed output in task space is geometrically an ellipsoid. This is shown and proven in section 2.1.1. The orientation and the radii of the volume bounded by the ellipsoid shows end-effector velocities (in task space) realizable by the manipulator.

If we denote the joint variables of a manipulator with n degrees of freedom by an n dimensional vector, \mathbf{q} and an m dimensional vector $\mathbf{r}=[r_1, K, r_m]^T$ to describe the position and/or orientation of the end-effector, then the kinematic relation between \mathbf{q} and \mathbf{r} is assumed to be:

$$\mathbf{r} = \mathbf{f}_r(\mathbf{q}) \quad (1.1)$$

we differentiate and get

$$\mathbf{v} = \mathbf{J}(\mathbf{q})\dot{\mathbf{q}} \quad (1.2)$$

Where $\mathbf{J}(\mathbf{q})$ is the jacobian matrix. Now we consider the set of all end-effector velocities \mathbf{v} which are realizable by joint velocities such that the euclidian norm of $\dot{\mathbf{q}}$,

$$\|\dot{\mathbf{q}}\| = \left(\sum_{i=1}^n \dot{q}_i^2 \right)^{1/2} \leq 1 \quad (1.3)$$

This set is an ellipsoid in m dimensional euclidian space. Since this ellipsoid represents the ability of manipulation, it is called the *manipulability ellipsoid*.

$$\dot{\mathbf{q}} = \mathbf{J}^+(\mathbf{q})\dot{\mathbf{r}} + (\mathbf{I} + \mathbf{J}^+(\mathbf{q})\mathbf{J}(\mathbf{q}))\mathbf{k} \quad (1.4)$$

$$\dot{\mathbf{q}}^T \dot{\mathbf{q}} = \dot{\mathbf{q}}^T \dot{\mathbf{q}} \quad (1.5)$$

every point in the ellipsoid holds $\|\dot{\mathbf{x}}\| \leq 1$. [1]

In his study Yoshikawa [1] shows that the direction of the principal axis of the manipulability ellipsoid is \mathbf{u}_i , and the radius in that direction is σ_i where subscript i denotes the dimension index and \mathbf{u}_i is the i -th column vector of matrix \mathbf{U} and σ_i is the i -th singular value in SVD form representation of manipulator jacobian. Figure below illustrates this property.

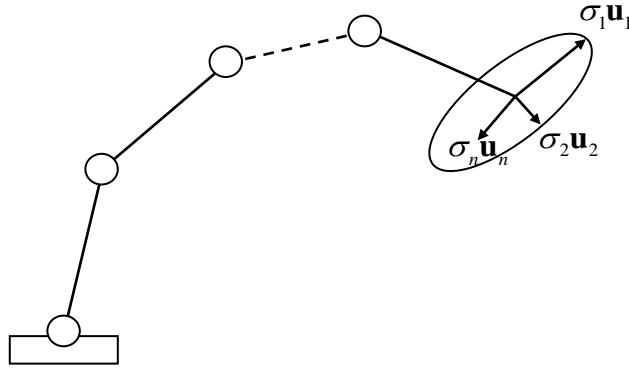


Figure 3.1: Manipulability ellipsoid of an arbitrary manipulator.

3.1.1. Singular Value Decomposition

For sets of equations that are either singular or else numerically very close to singularity where Gaussian elimination and LU decomposition fail, Singular Value Decomposition will diagnose the problem and in some cases it will also solve it, in the sense of giving a useful numerical answer. [5]

This subsection describes the singular value decomposition theorem and its proof [2], its relation with eigen-value decomposition theorem and geometrical interpretation [3].

SVD methods are based on the following theorem of linear algebra:

Let \mathbf{A} be a real $m \times n$ matrix. Then there exist orthogonal matrices \mathbf{U} and \mathbf{V} such that

$$\mathbf{U}^T \mathbf{A} \mathbf{V} = \begin{pmatrix} \mathbf{\Sigma}_1 & 0 \\ 0 & 0 \end{pmatrix} = \mathbf{\Sigma} \quad (1.6)$$

Where $\mathbf{\Sigma}_1$ is a nonsingular diagonal matrix. The diagonal entries of $\mathbf{\Sigma}$ are all nonnegative and can be arranged in nonincreasing order. Then number of nonzero diagonal entries of $\mathbf{\Sigma}$ equals the rank of \mathbf{A} . [2]

The geometrical interpretation of singular value decomposition shown by Strang [3] is represented in figure below.

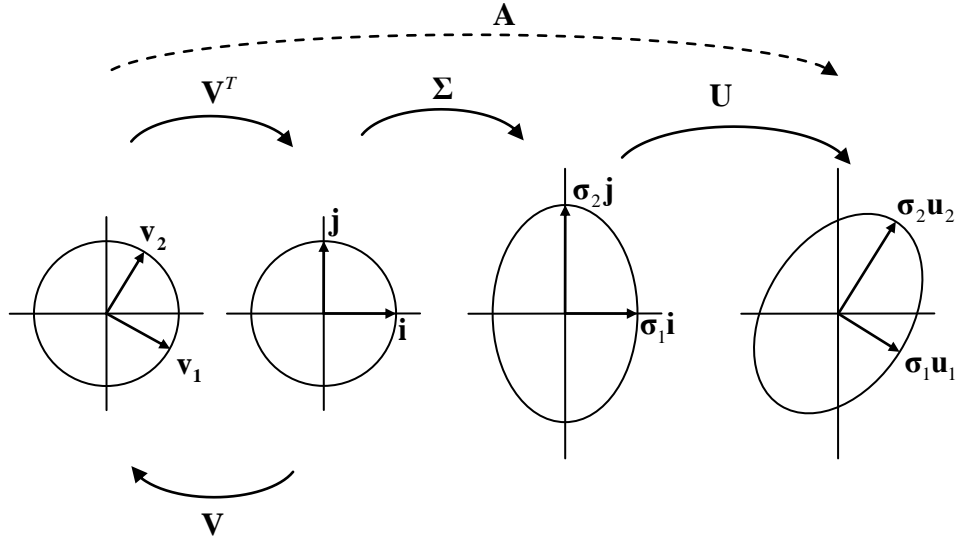


Figure 3.2: Geometrical representation of the singular value decomposition. \mathbf{U} and \mathbf{V} are rotations and reflections, $\mathbf{\Sigma}$ is a stretching matrix. [3]

To compute \mathbf{U} , $\mathbf{\Sigma}$ and \mathbf{V} matrices of SVD, we will use EVD described in section 3.1.2.

$$\mathbf{A} = \mathbf{U} \mathbf{\Sigma} \mathbf{V}^T \quad (1.7)$$

$$\begin{aligned} \mathbf{A} \mathbf{A}^T &= \mathbf{U} \mathbf{\Sigma} \mathbf{V}^T \mathbf{V} \mathbf{\Sigma}^T \mathbf{U}^T \\ &= \mathbf{U} \mathbf{\Sigma} \mathbf{\Sigma}^T \mathbf{U}^T \end{aligned} \quad (1.8)$$

$$\begin{aligned} \mathbf{A}^T \mathbf{A} &= \mathbf{V} \mathbf{\Sigma}^T \mathbf{U}^T \mathbf{U} \mathbf{\Sigma} \mathbf{V}^T \\ &= \mathbf{V} \mathbf{\Sigma}^T \mathbf{\Sigma} \mathbf{V}^T \end{aligned} \quad (1.9)$$

Then from (1.32), matrix \mathbf{U} is the eigen-vector matrix of $\mathbf{A}\mathbf{A}^T$, matrix \mathbf{V} is the eigen-vector matrix of $\mathbf{A}^T\mathbf{A}$ and finally matrix $\mathbf{\Sigma}$ is the diagonal matrix containing the square root of eigen-values of $\mathbf{A}\mathbf{A}^T$ or $\mathbf{A}^T\mathbf{A}$ as both are equal.

Before the proof of the SVD theorem we need to prove the theorem below:

Theorem 2.1: Let \mathbf{A} be a Hermitian matrix. Then,

1. There exists a unitary matrix \mathbf{U} such that

$$\mathbf{U}^*\mathbf{A}\mathbf{U} = \mathbf{D} \quad (1.10)$$

is a diagonal matrix.

2. The eigenvalues of \mathbf{A} are real.
3. The eigenvectors of \mathbf{A} may be chosen to be orthonormal.

Proof of 1: By the schur triangularization theorem we have

$$\mathbf{U}^*\mathbf{A}\mathbf{U} = \mathbf{T} \quad (1.11)$$

where \mathbf{T} is triangular. We now show that \mathbf{T} is diagonal. We have

$$(\mathbf{U}^*\mathbf{A}\mathbf{U})^* = \mathbf{T}^* \quad (1.12)$$

$$\mathbf{U}^*\mathbf{A}^*\mathbf{U} = \mathbf{T}^* \quad (1.13)$$

$$\mathbf{U}^*\mathbf{A}\mathbf{U} = \mathbf{T}^* \quad (\text{since } \mathbf{A}^* = \mathbf{A}) \quad (1.14)$$

$$\mathbf{T} = \mathbf{T}^* \quad (1.15)$$

This shows that \mathbf{T} is Hermitian. Because \mathbf{T} is triangular and Hermitian, it must be a diagonal matrix.

Proof of 2 : Because the eigenvalues of \mathbf{A} are the diagonal entries of \mathbf{T} and the diagonal entries of a Hermitian matrix must be real, it follows that the eigenvalues of \mathbf{A} are real.

Remark: Note that if \mathbf{A} is real, then $\mathbf{A}^* = \mathbf{A}$ implies that \mathbf{A} is symmetric ($\mathbf{A}^T = \mathbf{A}$). The eigen-values of a real symmetric matrix are also real.

Proof of 3 : Denote the columns of \mathbf{U} by \mathbf{u}_1 thorough \mathbf{u}_n , Then from

$$\mathbf{U}^*\mathbf{A}\mathbf{U} = \mathbf{D} \quad (1.16)$$

$$\mathbf{A}\mathbf{U} = \mathbf{U}\mathbf{D} \quad (1.17)$$

$$\mathbf{A}(\mathbf{u}_1, \mathbf{u}_2, \mathbf{K}, \mathbf{u}_n) = (\mathbf{u}_1, \mathbf{u}_2, \mathbf{K}, \mathbf{u}_n) \cdot \text{diag}(d_1, d_2, \mathbf{K}, d_n) \quad (1.18)$$

we see that \mathbf{u}_i is an eigenvector of \mathbf{A} corresponding to the eigenvalue d_i . Since \mathbf{U} is unitary, the eigenvectors $\mathbf{u}_1, \mathbf{u}_2, \dots, \mathbf{u}_n$ are orthonormal.

Let \mathbf{A} be real and symmetric, then, because its eigenvalues are real and eigenvectors can be chosen to be real, the unitary matrix \mathbf{U} in Theorem 2.1 can be orthogonal.

If \mathbf{A} is a real symmetric matrix, then there is an orthogonal matrix \mathbf{U} such that $\mathbf{U}^T \mathbf{A} \mathbf{U} = \mathbf{D}$, where \mathbf{D} is diagonal. [2]

Proof of SVD Theorem :

Consider the matrix $\mathbf{A}^T \mathbf{A}$. It is an $n \times n$ symmetric positive semidefinite matrix; therefore its eigenvalues are nonnegative. Denote the eigenvalues of $\mathbf{A}^T \mathbf{A}$ by $\lambda_1 = \sigma_1^2, \lambda_1 = \sigma_1^2, \dots, \lambda_r = \sigma_r^2$. Assume that these have been ordered such that $\sigma_1 \geq \sigma_2 \geq \dots \geq \sigma_r > 0$, and $\sigma_{r+1} = \sigma_{r+2} = \dots = \sigma_n = 0$

Above we have proved that a symmetric matrix has a set of orthonormal eigenvectors. Denote the set of orthonormal eigenvectors of $\mathbf{A}^T \mathbf{A}$ corresponding to λ_1 through λ_n by $\mathbf{v}_1, \dots, \mathbf{v}_n$: that is, \mathbf{v}_1 through \mathbf{v}_n are orthonormal and satisfy

$$\mathbf{A}^T \mathbf{A} \mathbf{v}_i = \sigma_i^2 \mathbf{v}_i, \quad i = 1, \dots, n \quad (1.19)$$

$$\mathbf{v}_i^T \mathbf{A}^T \mathbf{A} \mathbf{v}_i = \sigma_i^2 \neq 0, \quad i = 1, \dots, r \quad (1.20)$$

$$\mathbf{v}_i^T \mathbf{A}^T \mathbf{A} \mathbf{v}_j = 0, \quad i = 1, \dots, r; j \neq i \quad (1.21)$$

$$\mathbf{V}_1 = (\mathbf{v}_1, \dots, \mathbf{v}_r) \quad (1.22)$$

$$\mathbf{V}_2 = (\mathbf{v}_{r+1}, \dots, \mathbf{v}_n) \quad (1.23)$$

where \mathbf{v}_1 through \mathbf{v}_r are the eigenvectors associated with the nonzero eigenvalues λ_1 through λ_r and $\mathbf{v}_{r+1}, \dots, \mathbf{v}_n$ correspond to the zero eigenvalues. Then

$$\mathbf{V}_2^T \mathbf{A}^T \mathbf{A} \mathbf{V}_2 = \mathbf{V}_2 \mathbf{A}^T \mathbf{A} (\mathbf{v}_{r+1}, \dots, \mathbf{v}_n) = \mathbf{V}_2^T (0, 0, \dots, 0) = 0 \quad (1.24)$$

This implies that $\mathbf{A} \mathbf{V}_2 = 0$, or

$$\mathbf{A} \mathbf{v}_k = 0, \quad k = r+1, r+2, \dots, n \quad (1.25)$$

Define now a set of nonzero vectors $\{\mathbf{u}_i\}$ by

$$\mathbf{u}_i = \frac{1}{\sigma_i} \mathbf{A} \mathbf{v}_i, \quad i=1, K, r \quad (1.26)$$

The \mathbf{u}_i 's $i=1, K, r$, then form an orthonormal set, because

$$\begin{aligned} \mathbf{u}_i^T \mathbf{u}_j &= \frac{1}{\sigma_i} (\mathbf{A} \mathbf{v}_i)^T \frac{1}{\sigma_j} (\mathbf{A} \mathbf{v}_j) \\ &= \frac{1}{\sigma_i \sigma_j} (\mathbf{v}_i^T \mathbf{A}^T \mathbf{A} \mathbf{v}_j) \\ &= \begin{cases} 0 & \text{when } i \neq j \\ 1 & \text{when } i = j \end{cases} \end{aligned} \quad (1.27)$$

Define $\mathbf{U}_1 = (\mathbf{u}_1, K, \mathbf{u}_r)$, and choose $\mathbf{U}_2 = (\mathbf{u}_{r+1}, K, \mathbf{u}_n)$ such that $\mathbf{U} = (\mathbf{U}_1, \mathbf{U}_2)$ is orthogonal. Then, for any $k > r$, we have

$$\mathbf{u}_k^T \mathbf{A} \mathbf{v}_i = \sigma_i \mathbf{u}_k^T \mathbf{u}_i = 0, \quad i=1, K, r \quad (\text{Note that by (1.26), } \mathbf{A} \mathbf{v}_i = \sigma_i \mathbf{u}_i)$$

(by orthogonality of the vectors of \mathbf{U}), and

$$\mathbf{u}_k^T \mathbf{A} \mathbf{v}_i = 0, \quad i=r+1, K, n \quad (1.28)$$

by (1.25).

Let $\mathbf{V} = (\mathbf{V}_1, \mathbf{V}_2)$, then

$$\begin{aligned} \mathbf{U}^T \mathbf{A} \mathbf{V} &= \begin{pmatrix} \mathbf{u}_1^T \\ \mathbf{u}_2^T \\ \mathbf{M} \\ \mathbf{u}_m^T \end{pmatrix} \mathbf{A} (\mathbf{v}_1, K, \mathbf{v}_n) = \begin{pmatrix} \frac{1}{\sigma_1} \mathbf{v}_1^T \mathbf{A}^T \\ \frac{1}{\sigma_1} \mathbf{v}_1^T \mathbf{A}^T \\ \mathbf{M} \\ \frac{1}{\sigma_1} \mathbf{v}_1^T \mathbf{A}^T \\ \mathbf{u}_{r+1}^T \\ \mathbf{M} \\ \mathbf{u}_m^T \end{pmatrix} \mathbf{A} (\mathbf{v}_1, K, \mathbf{v}_n) \\ &= \begin{pmatrix} \frac{1}{\sigma_1} \cdot \sigma_1^2 & & & & & & 0 \\ & \frac{1}{\sigma_2} \cdot \sigma_2^2 & & & & & \\ & & \ddots & & & & \\ & & & \mathbf{O} & & & \\ & & & & \frac{1}{\sigma_r} \cdot \sigma_r^2 & & \\ 0 & & & & & & 0 \end{pmatrix} = \mathbf{\Sigma} = \begin{pmatrix} \mathbf{\Sigma}_1 & 0 \\ 0 & 0 \end{pmatrix} \end{aligned} \quad (1.29)$$

where $\mathbf{\Sigma}_1 = \text{diag}(\sigma_1, K, \sigma_r)$

The statement about the rank is obvious, $\text{rank}(\mathbf{A}) = \text{rank}(\mathbf{U}\mathbf{\Sigma}\mathbf{V}^T) = \text{rank}(\mathbf{\Sigma}) = r$.

The decomposition $\mathbf{A} = \mathbf{U}\mathbf{\Sigma}\mathbf{V}^T$ is known as the singular value decomposition (SVD) of \mathbf{A} .

The diagonal entries of the matrix $\mathbf{\Sigma}$ are called the **singular values** of \mathbf{A} . The numbers $\sigma_1, \sigma_2, \dots, \sigma_r$ are the positive singular values of \mathbf{A} .

The columns of \mathbf{U} are called **left singular vectors** and those of \mathbf{V} are called **right singular vectors**. [2]

Uniqueness of the Singular Value Decomposition

There are $k = \min(m, n)$ singular values of \mathbf{A} . Let r be the rank of \mathbf{A} . Then there are r positive singular values. These are the positive square roots of the nonzero eigen-values of $\mathbf{A}^T \mathbf{A}$ (of $\mathbf{A} \mathbf{A}^T$). The remaining $(k - r)$, if $r < k$, singular values are zero. Thus, the singular values are unique. However, the singular vectors are not unique. For example, if \mathbf{A} has a multiple singular value $\sigma > 0$, then the corresponding columns of the matrix \mathbf{V} can be chosen as any orthonormal basis of the space spanned by the eigenvectors associated with the multiple eigenvalue $\lambda = \sigma^2$ of $\mathbf{A}^T \mathbf{A}$. [2]

3.1.2. Diagonalization of a matrix

Let \mathbf{S} be a matrix whose columns are the n linearly independent eigenvectors of a matrix $\mathbf{A} \in R^{n \times n}$ and let $\mathbf{\Lambda}$ be eigenvalue matrix of \mathbf{A} with

$$\Lambda_{ij} = \begin{cases} \lambda_i \text{ of } \mathbf{A}, & \text{if } i = j \\ 0, & \text{if } i \neq j \end{cases} \quad (1.30)$$

$$\begin{aligned} \mathbf{AS} &= \mathbf{A} [\mathbf{x}_1, \dots, \mathbf{x}_n] = [\lambda_1 \mathbf{x}_1, \dots, \lambda_n \mathbf{x}_n] \\ &= [\mathbf{x}_1, \dots, \mathbf{x}_n] \begin{bmatrix} \lambda_1 & & 0 \\ & \mathbf{O} & \\ 0 & & \lambda_n \end{bmatrix} = \mathbf{S}\mathbf{\Lambda} \end{aligned} \quad (1.31)$$

$$\mathbf{A} = \mathbf{S}\mathbf{\Lambda}\mathbf{S}^{-1} \quad (1.32)$$

[3]

3.1.3. Pseudo-inverse.

In robotics, inverting singular and/or non-square matrices is necessary in cases like identification of manipulator dynamics and control of redundant manipulators. That's why a more general inversion named *pseudoinverse* is employed in these cases. [1]

Let \mathbf{A}^+ denote the generalized inverse of \mathbf{A} , if

$$\mathbf{A}\mathbf{A}^+\mathbf{A} = \mathbf{A} \quad (1.33)$$

then \mathbf{A}^+ is said to be a *generalized inverse* of \mathbf{A} . If a generalized inverse also satisfies

$$\mathbf{A}^+\mathbf{A}\mathbf{A}^+ = \mathbf{A}^+ \quad (1.34)$$

then \mathbf{A}^+ is a *reflexive generalized inverse*. A reflexive generalized inverse with

$$(\mathbf{A}^+\mathbf{A})^* = \mathbf{A}^+\mathbf{A} \quad (1.35)$$

is called as a *left weak generalized inverse*. Finally a *pseudo-inverse* or *Moore-Penrose generalized inverse* \mathbf{A}^+ of a matrix \mathbf{A} is a left-weak generalized inverse which also holds for

$$(\mathbf{A}\mathbf{A}^+)^* = \mathbf{A}\mathbf{A}^+ \quad (1.36)$$

Where $*$ denotes complex conjugate transpose (hermitian). The generalized inverse covers ordinary inverse of square non-singular matrices so that $\mathbf{A}^+ = \mathbf{A}^{-1}$

[4]

For every finite $m \times n$ real matrix \mathbf{A} , there is a unique $n \times m$ real matrix \mathbf{A}^+ satisfying (1.33), (1.34), (1.35) and (1.36).

Proof of existence:

Let \mathbf{A} be an $m \times n$ real matrix. If $\mathbf{A} = 0$, then $\mathbf{A}^+ = 0$ is an obvious solution of equations (1.33) to (1.36). If we assume $\mathbf{A} \neq 0$ and decompose \mathbf{A} to multiplication of $m \times r$ matrix \mathbf{B} and $r \times n$ matrix \mathbf{C} , where $r = \text{rank}\mathbf{A}$, in form,

$$\mathbf{A} = \mathbf{B}\mathbf{C} \quad (1.37)$$

$$\mathbf{A}^+ = \mathbf{C}^T(\mathbf{C}\mathbf{C}^T)^{-1}(\mathbf{B}^T\mathbf{B})^{-1}\mathbf{B}^T \quad (1.38)$$

Satisfies equations (1.33) to (1.36) and this proves the existense of pseudoinverse.

Proof of uniqueness:

Let any two matrices \mathbf{A}_1^+ and \mathbf{A}_2^+ satisfy equations (1.33) to (1.36). Then,

$$\mathbf{A}_1^+ - \mathbf{A}_2^+ = \mathbf{A}_1^+ \mathbf{A} \mathbf{A}_1^+ - \mathbf{A}_2^+ \mathbf{A} \mathbf{A}_2^+ \quad (1.39)$$

If we substitute $\mathbf{A}_1^+ \mathbf{A}$ with $\mathbf{A}^T \mathbf{A}_1^{+T}$ using (1.36) and $\mathbf{A} \mathbf{A}_2^+$ with $\mathbf{A}_2^{+T} \mathbf{A}^T$ using (1.35) then,

$$= \mathbf{A}^T \mathbf{A}_1^{+T} \mathbf{A}_1^T - \mathbf{A}_2^+ \mathbf{A}_2^{+T} \mathbf{A}^T \quad (1.40)$$

Using equation (1.33) we replace \mathbf{A}_i^T with $\mathbf{A} \mathbf{A}_{3-i}^+ \mathbf{A}$ for $i = \{1, 2\}$,

$$= (\mathbf{A} \mathbf{A}_2^+ \mathbf{A})^T \mathbf{A}_1^{+T} \mathbf{A}_1^+ - \mathbf{A}_2^+ \mathbf{A}_2^{+T} (\mathbf{A} \mathbf{A}_1^+ \mathbf{A})^T \quad (1.41)$$

$$= \mathbf{A}^T \mathbf{A}_2^{+T} \mathbf{A}^T \mathbf{A}_1^{+T} \mathbf{A}_1^+ - \mathbf{A}_2^+ \mathbf{A}_2^{+T} \mathbf{A}^T \mathbf{A}_1^+ \mathbf{A}^T \quad (1.42)$$

Next we substitute $\mathbf{A}^T \mathbf{A}_1^{+T} \mathbf{A}_1^+$ with \mathbf{A}_1^+ using (1.34), (1.36) and $\mathbf{A}_2^+ \mathbf{A}_2^{+T} \mathbf{A}^T$ with \mathbf{A}_2^+ using (1.34) and (1.35),

$$= \mathbf{A}^T \mathbf{A}_2^{+T} \mathbf{A}_1^+ - \mathbf{A}_2^+ \mathbf{A}_1^{+T} \mathbf{A}^T \quad (1.43)$$

Finally $\mathbf{A}^T \mathbf{A}_2^{+T}$ is replaced with $\mathbf{A}_2^+ \mathbf{A}$ using (1.36) and $\mathbf{A}_1^{+T} \mathbf{A}^T$ with $\mathbf{A} \mathbf{A}_1^+$,

$$\mathbf{A}_1^+ - \mathbf{A}_2^+ = \mathbf{A}_2^+ \mathbf{A} \mathbf{A}_1^+ - \mathbf{A}_2^+ \mathbf{A} \mathbf{A}_1^+ = 0 \quad (1.44)$$

This proves the uniqueness of the pseudoinverse.

[1]

3.1.4. Formulating the Null-Space of a Matrix

Let an n -dimensional subspace S is spanned by n linearly independent vectors $\mathbf{a}_i, i=1 \dots n$ and let vector $\bar{\mathbf{x}}$ denote the closest point to vector \mathbf{k} in subspace S .

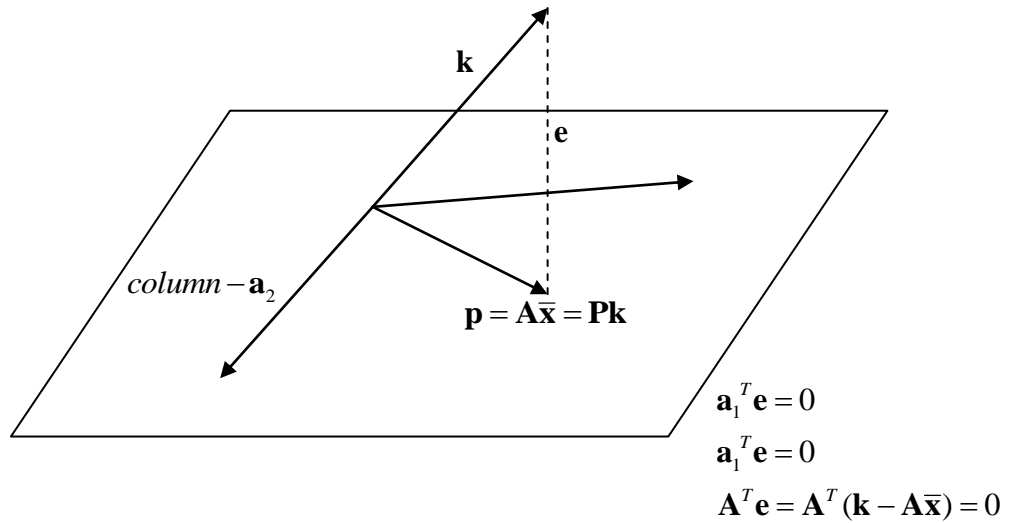


Figure 3.3: Projection of a vector onto a subspace

The error vector $\mathbf{k} - \bar{\mathbf{x}}$ is perpendicular to the subspace S to,

$$\mathbf{a}_i^T (\mathbf{k} - \mathbf{Ax}) = 0$$

$$\begin{bmatrix} \mathbf{a}_1^T \\ \vdots \\ \mathbf{a}_n^T \end{bmatrix} \mathbf{M} [\mathbf{k} - \mathbf{Ax}] = [0] \quad (1.45)$$

$$\mathbf{A}^T (\mathbf{k} - \mathbf{Ax}) = 0$$

$$\mathbf{A}^T \mathbf{Ax} = \mathbf{A}^T \mathbf{k}, \mathbf{x} = (\mathbf{A}^T \mathbf{A})^{-1} \mathbf{A}^T \mathbf{k}$$

Then the projection matrix that produces $\mathbf{p} = \mathbf{Pk}$ is

$$\mathbf{P} = \mathbf{A}(\mathbf{A}^T \mathbf{A})^{-1} \mathbf{A}^T \quad (1.46)$$

[3]

Null-space of a matrix \mathbf{A} can be expressed as the union of all error vectors,

$$\begin{aligned} \mathbf{e} &= \mathbf{k} - \mathbf{Ax} \\ &= (\mathbf{I} - \mathbf{P})\mathbf{k} \\ &= (\mathbf{I} - \mathbf{A}(\mathbf{A}^T \mathbf{A})^{-1} \mathbf{A}^T)\mathbf{k} \\ &= (\mathbf{I} - \mathbf{AA}^+)\mathbf{k} \end{aligned} \quad (1.47)$$

where \mathbf{k} is an arbitrary vector.

3.1.5. Generalized Solution

The generalized solution of a system of simultaneous linear equations given by $\mathbf{Ax} = \mathbf{b}$, if $\mathbf{b} \in \mathbf{R}(\mathbf{A})$, Then

$$\mathbf{x} = \mathbf{A}^+ \mathbf{b} + \mathbf{h} \quad (1.48)$$

Where \mathbf{h} is any vector in the null-space of \mathbf{A}^+ . Then using eq.1 the generalized solution is

$$\mathbf{x} = \mathbf{A}^+ \mathbf{b} + (\mathbf{I} - \mathbf{AA}^+)\mathbf{k} \quad (1.49)$$

where \mathbf{k} is an arbitrary vector.

3.2. Manipulability Polytope

Manipulability ellipsoid approach derives its output from a region in joint velocity space described by $\|\dot{\mathbf{q}}\|_2 \leq 1$ which does not transform the exact joint constraints. A more accurate definition is $\|\dot{\mathbf{q}}\|_\infty = \max_i |\dot{q}_i| \leq \dot{q}_{\max}$ (l_∞ norm sense). In this section, computation of polytope vertices corresponding to the constraints given in joint space are derived. If we rearrange $\mathbf{v} = \mathbf{J}(\mathbf{q})\dot{\mathbf{q}}$ as

$$\begin{aligned} \mathbf{v} &= (\mathbf{j}_1, \dots, \mathbf{j}_n)(\dot{q}_1, \dots, \dot{q}_n) \\ &= \sum_{i=1}^n \dot{q}_i \mathbf{j}_i \end{aligned} \quad (1.50)$$

Where \mathbf{j}_i is the i -th column vector of \mathbf{J} , we can interpret the \mathbf{v} as a linear combination of column vectors of \mathbf{J} with coefficients whose bounds are given by $|\dot{q}_i| \leq 1$.

[6]

3.2.1. Computation of vertices:

Pseudo-code of the algorithm for computing the vertices of the polytope derived from initial manipulator jacobian is listed below.

```

Array=zeros_vector
For each column j in manipulator jacobian:
    for each vector v in Array:
        new_array.insert v+j
        new_array.insert v-j
    end
end
Array=new_array.
Array.remove_interior_vertices.

```

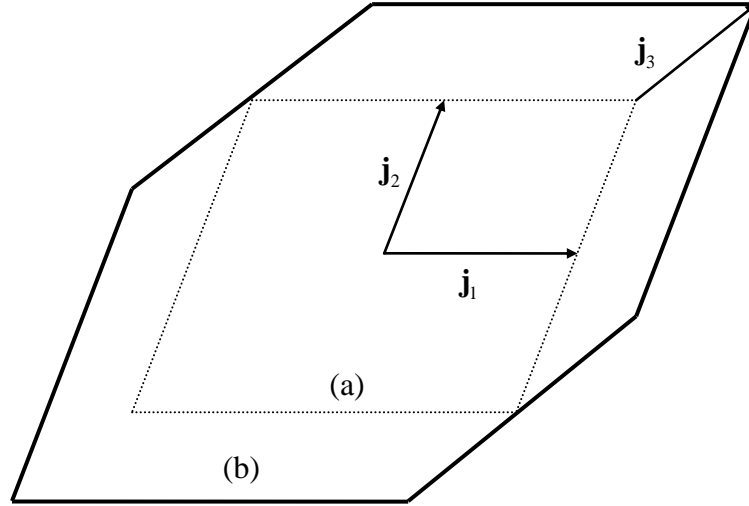



Figure 3.4: Construction of manipulability polytopes in 2-dimensional task space for a 3 joint robot. (a) Polytope made of two vectors. (b) Polytope after adding one more vector.

3.2.2. Derivation of a Manipulability Index Based on Polytope

Let $\mathbf{V}_j, j=1, K, N_v$ be the vectors representing the vertices of a polytope in n -dimensional task space, and N_v be the count of vertices. Then a vector set $\{\mathbf{V}_{k_i}, i=1, K, n\}$ is called primary vertex set if there are no elements of the polytope represented by

$$\sum_{i=1}^n \lambda_{k_i} \mathbf{V}_{k_i}, \lambda_{k_i} \geq 0, \sum_{i=1}^n \lambda_{k_i} > 1 \quad (1.51)$$

the region described by the following equation is called Cone-cell_K.

$$\sum_{i=1}^n \lambda_{k_i} \mathbf{V}_{k_i}, \lambda_{k_i} \geq 0, \sum_{i=1}^n \lambda_{k_i} \leq 1 \quad (1.52)$$

and the plane described by

$$\sum_{i=1}^n \lambda_{k_i} \mathbf{V}_{k_i}, \lambda_{k_i} \geq 0, \sum_{i=1}^n \lambda_{k_i} = 1 \quad (1.53)$$

is called the bottom plane of Cone-cell_K.

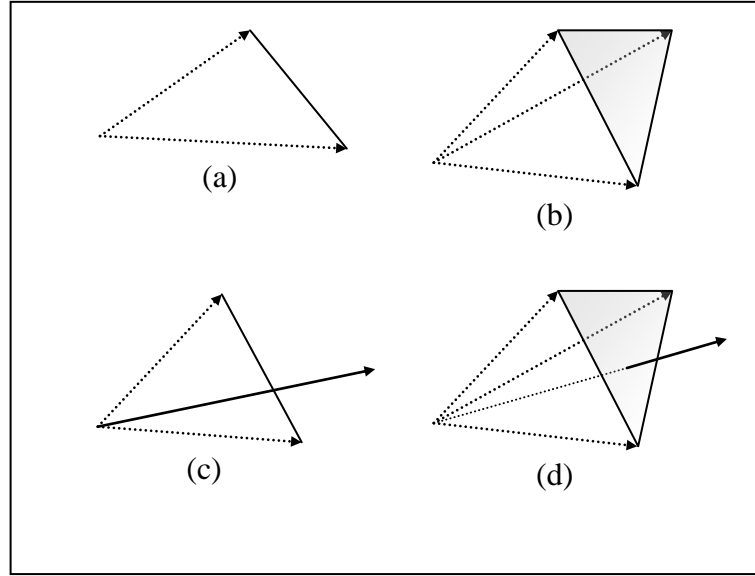


Figure 3.5: Examples of Cone-cell in (a) 2-dimensional task space and (b) 3 dimensional task space and non-Con-cell in (c) 2-dimensional task space and (d) 3 dimensional task-space.

If we denote the volume of the k-th cone-cell as S_k then

$$S_k = \frac{1}{d_n} \left| \det \left(\begin{bmatrix} \mathbf{V}_{k_1} & \mathbf{K} & \mathbf{V}_{k_n} \end{bmatrix} \right) \right|, \quad (1.54)$$

where d_n is a constant determined by the dimension of task space [10]. Note that

$\begin{bmatrix} \mathbf{V}_{k_1} & \mathbf{K} & \mathbf{V}_{k_n} \end{bmatrix}$ is $n \times n$ square matrix. With above equation for volume, we define a

manipulability measure related to the ability of moving along arbitrary direction as

$$w_p = \sum S_k \quad (1.55)$$

[6]

4. Simulation Results

4.1. Computation of manipulator Jacobian

This section describes the formulation used for the computation of manipulator jacobian used in the computation of manipulability ellipsoid and manipulability polytopes.

Let ω_i denotes angular velocity of origin of joint i, \mathbf{v}_i denotes linear velocity of

origin of joint i and $\mathbf{V}_i = \begin{bmatrix} \omega_i \\ \mathbf{v}_i \end{bmatrix}$ denotes the spatial velocity.

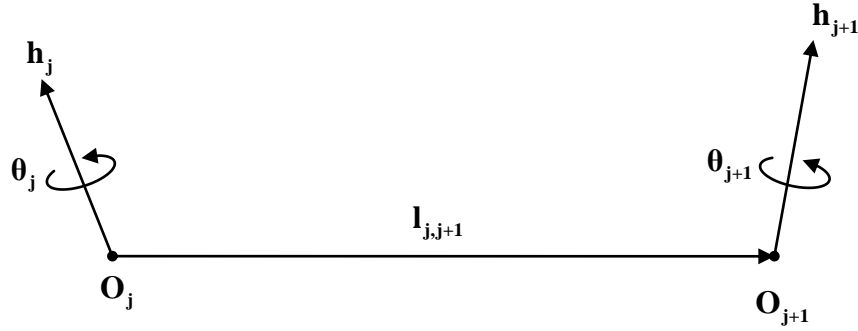


Figure 4.1: Geometric layout of links and \mathbf{h} vectors.

$$\omega_j = \omega_{j-1} + \mathbf{h}_k \dot{\theta}_k \quad (1.56)$$

$$\mathbf{v}_j = \mathbf{v}_{j-1} + \omega_{j-1} \times \mathbf{l}_{j-1,j}$$

$$\text{If we denote } \hat{\mathbf{x}} = \begin{bmatrix} 0 & -x_3 & x_2 \\ x_3 & 0 & -x_1 \\ -x_2 & x_1 & 0 \end{bmatrix} \quad (1.57)$$

The cross-product of two vectors \mathbf{x} and \mathbf{y} can also be formulated in form,

$$\mathbf{x} \times \mathbf{y} = \begin{bmatrix} 0 & -x_3 & x_2 \\ x_3 & 0 & -x_1 \\ -x_2 & x_1 & 0 \end{bmatrix} \begin{bmatrix} y_1 \\ y_2 \\ y_3 \end{bmatrix} = \hat{\mathbf{x}} \mathbf{y} \quad (1.58)$$

Then

$$\begin{aligned}
\mathbf{v}_j &= \mathbf{v}_{j-1} - \hat{\mathbf{l}}_{j-1,j} \times \boldsymbol{\omega}_{j-1} \\
&= \mathbf{v}_{j-1} - \hat{\mathbf{l}}_{j-1,j} \boldsymbol{\omega}_{j-1}
\end{aligned} \tag{1.59}$$

So in matrix form,

For a revolute joint

$$\begin{bmatrix} \boldsymbol{\omega}_j \\ \mathbf{v}_j \end{bmatrix} = \begin{bmatrix} \mathbf{I} & 0 \\ -\hat{\mathbf{l}}_{j-1,j} & \mathbf{I} \end{bmatrix} \begin{bmatrix} \boldsymbol{\omega}_{j-1} \\ \mathbf{v}_{j-1} \end{bmatrix} + \begin{bmatrix} \mathbf{h}_j \\ \mathbf{0} \end{bmatrix} \dot{\theta}_j \tag{1.60}$$

$$\mathbf{V}_j = \boldsymbol{\phi}_{j,j-1} \mathbf{V}_{j-1} + \mathbf{H}_j \dot{\boldsymbol{\theta}}_j \tag{1.61}$$

$$\begin{bmatrix} \mathbf{V}_1 \\ \mathbf{V}_2 \\ \mathbf{V}_3 \\ \mathbf{M} \\ \mathbf{V}_n \end{bmatrix} = \begin{bmatrix} \mathbf{I} & & \mathbf{L} & & 0 \\ \mathbf{f}_{2,1} & \mathbf{I} & & & \\ \mathbf{f}_{3,1} & \mathbf{f}_{3,2} & \mathbf{I} & & \mathbf{M} \\ \mathbf{M} & & & \mathbf{O} & \\ \mathbf{f}_{n,1} & \mathbf{f}_{n,2} & \mathbf{L} & \mathbf{f}_{n,n-1} & \mathbf{I} \end{bmatrix} \begin{bmatrix} \mathbf{H}_1 \boldsymbol{\theta}_1 \\ \mathbf{H}_2 \boldsymbol{\theta}_2 \\ \mathbf{H}_3 \boldsymbol{\theta}_3 \\ \mathbf{M} \\ \mathbf{H}_n \boldsymbol{\theta}_n \end{bmatrix} \tag{1.62}$$

$$\mathbf{V}_n(\mathbf{q}, \dot{\mathbf{q}}) = \begin{bmatrix} \boldsymbol{\phi}_{n,1} & \boldsymbol{\phi}_{n,2} & \mathbf{L} & \boldsymbol{\phi}_{n,n} \end{bmatrix} \begin{bmatrix} \mathbf{H}_1 \boldsymbol{\theta}_1 \\ \mathbf{M} \\ \mathbf{H}_n \boldsymbol{\theta}_n \end{bmatrix}$$

$$\begin{aligned}
\boldsymbol{\sigma}_t &= \begin{bmatrix} 0 & 0 & \mathbf{K} & \phi_{t,n} \end{bmatrix} \\
\mathbf{V}_t &= \boldsymbol{\sigma}_t \mathbf{V} \\
\mathbf{V}_t &= \boldsymbol{\sigma}_t \boldsymbol{\phi} \mathbf{H} \dot{\boldsymbol{\theta}} = \mathbf{J} \dot{\boldsymbol{\theta}} \\
\mathbf{J} &= \boldsymbol{\sigma}_t \boldsymbol{\phi} \mathbf{H}
\end{aligned} \tag{1.63}$$

4.2. Results from manipulability ellipsoids and manipulability polytopes with comparative results.

This section contains the plots of case studies used for comparison of the manipulability ellipsoid and manipulability polytope approaches. Three type of manipulators are chosen to populate the result set and for simplicity only translational results are drawn in the plots.

The first type of manipulator is a simple 2 link planar arm with no redundancy. Its links are length of 1 unit. Figure below shows the translation manipulability polytope of this manipulator for both joint angles of $\pi/4$. Its in shape of a parallelogram and this parallelogram gets narrower and close to a form of line as joint angles get closer to 0.

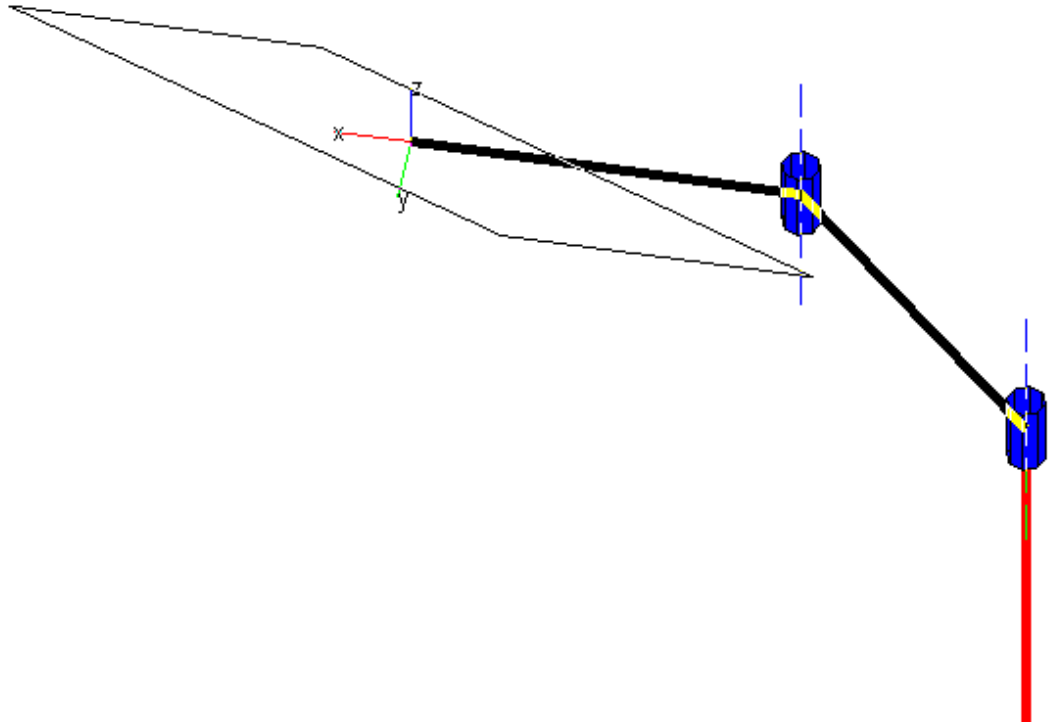


Figure 4.2: Manipulability polytope of a two link planar arm.

Figure below illustrates both the manipulability polytope and manipulability ellipsoids for the 2 link planar arm for the same configuration. The edges of the polytope is tangential to the ellipsoid and covers a wider solution set.

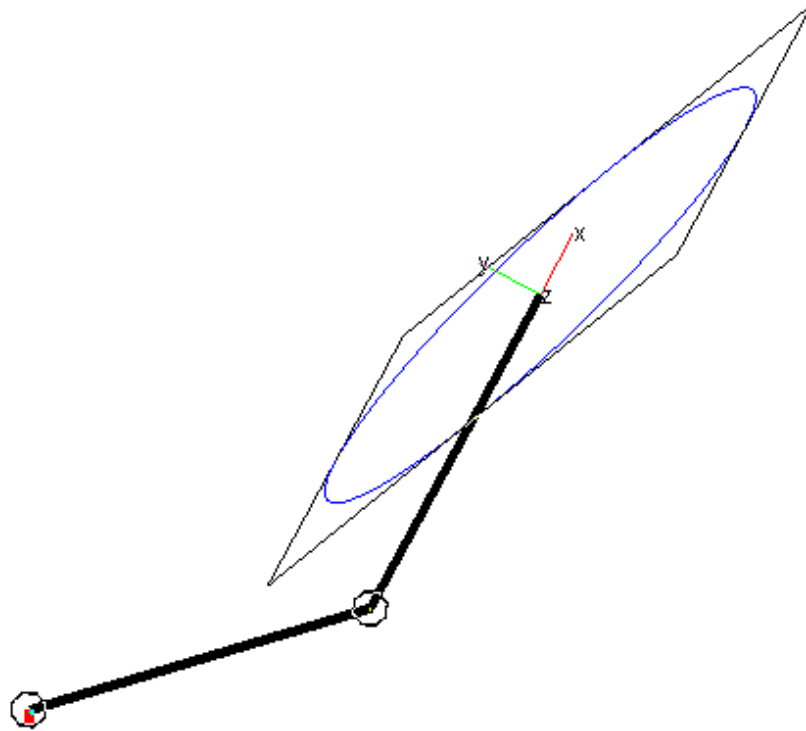


Figure 4.3: Manipulability ellipsoid and polytope of a two link planar arm for the same configuration

Figure below plots the translational manipulability ellipsoid and manipulability polytopes of MPA10 robot arm for configuration vector

$$\mathbf{q} = [0 \quad \pi/4 \quad 0 \quad \pi/4 \quad 0 \quad \pi/4 \quad 0].$$

In this configuration the polytope is in shape of extrusion of an improper hexagon and ellipsoid covers a smaller volume while orientations of the polytope and ellipsoid are equal.

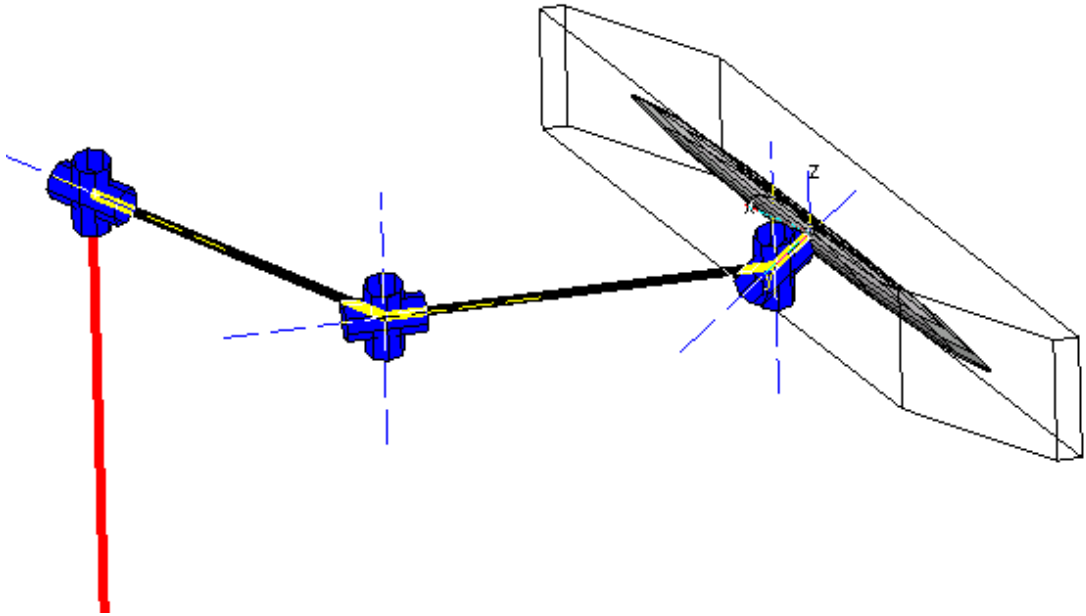


Figure 4.4: Manipulability ellipsoid and polytope of a MPA10 for the same joint configuration.

Last case is for a P560 type robot manipulator. Figure below shows both the manipulability ellipsoid and manipulability polytope for configuration vector $\mathbf{q} = [\pi/4 \ \pi/4 \ \pi/4 \ \pi/4 \ \pi/4 \ \pi/4]$

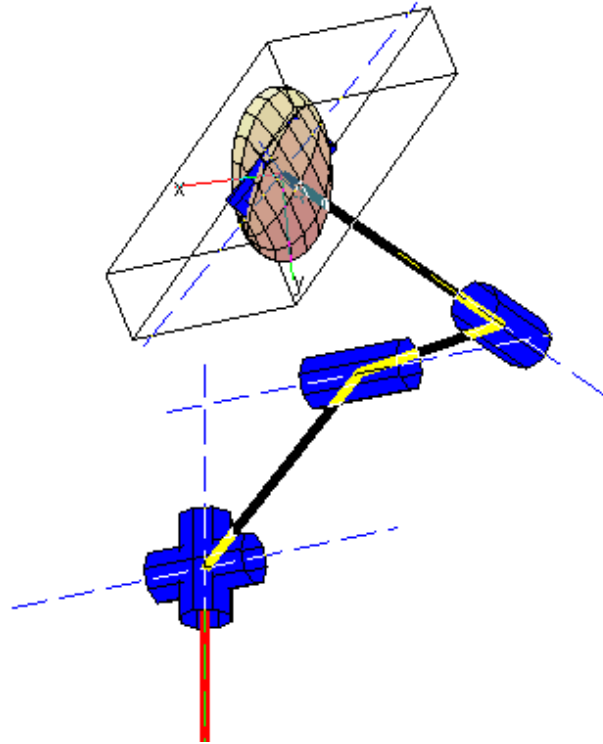


Figure 4.5: Manipulability ellipsoid and polytope of a P560 for the same configuration.

This case also shows that the manipulability polytope covers a wider solution set than the manipulability ellipsoid.

5. Conclusion

In this study the control of redundant manipulators using task decomposition approach, manipulability measures for redundant and non-redundant manipulators are examined. Manipulability ellipsoid and manipulability polytope approaches and their formulation are described. Singular value decomposition theorem which is used in finding the axes of manipulability polytope is described, its existence and uniqueness are proven. Generalized Moore-Penrose inverse (pseudo-inverse) of a matrix is described, its existence and uniqueness is proven. Eigen-value decomposition which is used in computation of singular value decomposition, and generalized solution of simultaneous linear equations employed in calculations of task decomposition and manipulability ellipsoid methods are described.

Finally both manipulability measures are illustrated for three types of manipulators. Plots are generated with MATLAB r14 using the Robotics toolbox and MPT toolbox which are freely downloadable on internet.

As a future study this text is planned to be expanded from kinematic aspect to dynamical aspect. Further, for experimenting the results obtained on MPA10, a driver application that will communicate with the robot arm via ARCNET protocol is being developed. Some of the UML diagrams of this application are illustrated in Appendix-A.

References

- [1] **Yoshigawa, T.**, 1990. Foundations of Robotics, Analysis and Control. MIT Press
- [2] **Nath Datta B.**, 1995. Numerical Linear Algebra and Applications, Brooks/Cole Publishing Company.
- [3] **Strang G.**, 2003. Introduction to Linear Algebra. Wellesley-Cambridge Press
- [4] **Teresa Ge K.**, 2000. Solving Inverse Kinematics Constraint Problems for Highly Articulated Models.
- [5] **William H. Press, Brian P. Flannery, Saul A. Teukolsky, William T. Vetterling**, 1992. Numerical Recipes in C: The art of scientific computing, Cambridge University Press; 2 edition.
- [6] **Lee, J.**, A Study on the Manipulability Measures for Robot Manipulators.
- [7] **Liegeois A.**, “Automatic Supervisory Control of the configuration and behavior of multibody mechanisms,” IEEE Transactions on Systems, Man, and Cybernetics 7, no 12 (1977), 868-871.

Appendix A. UML Diagrams of the communications library

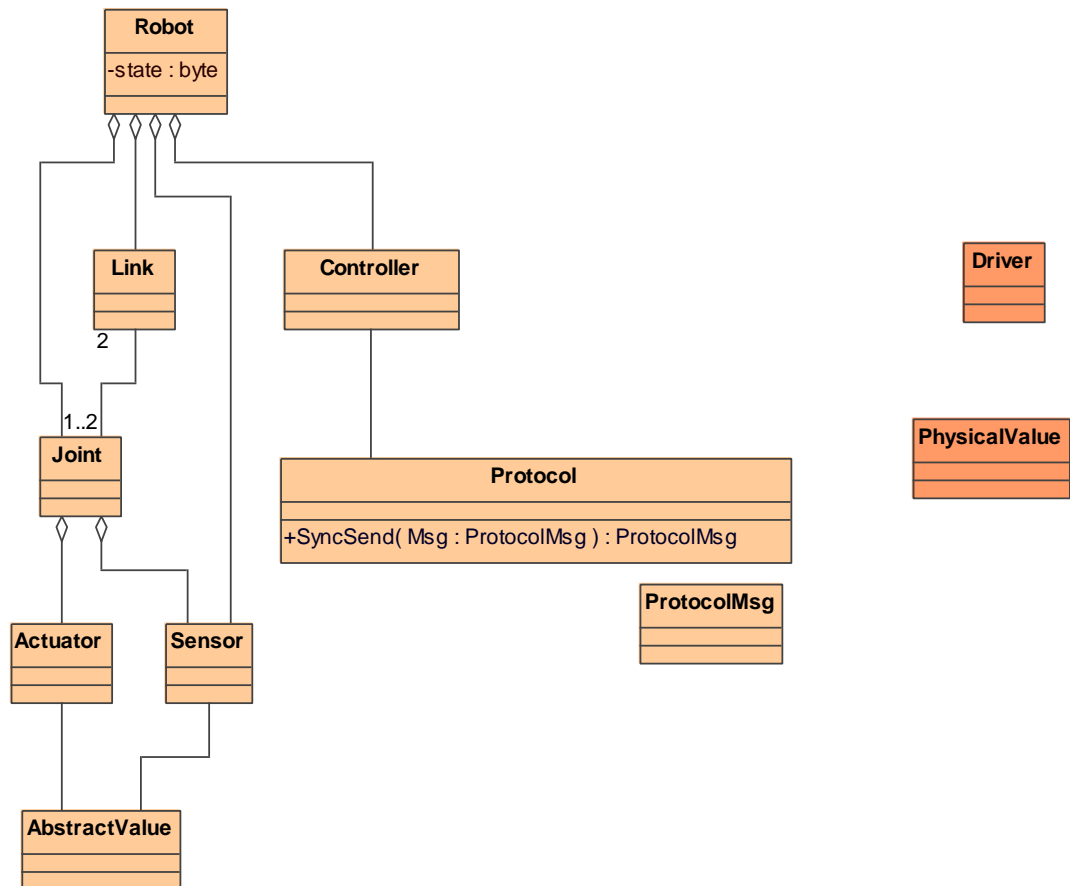


Figure A.1: Class diagram for the irlroot

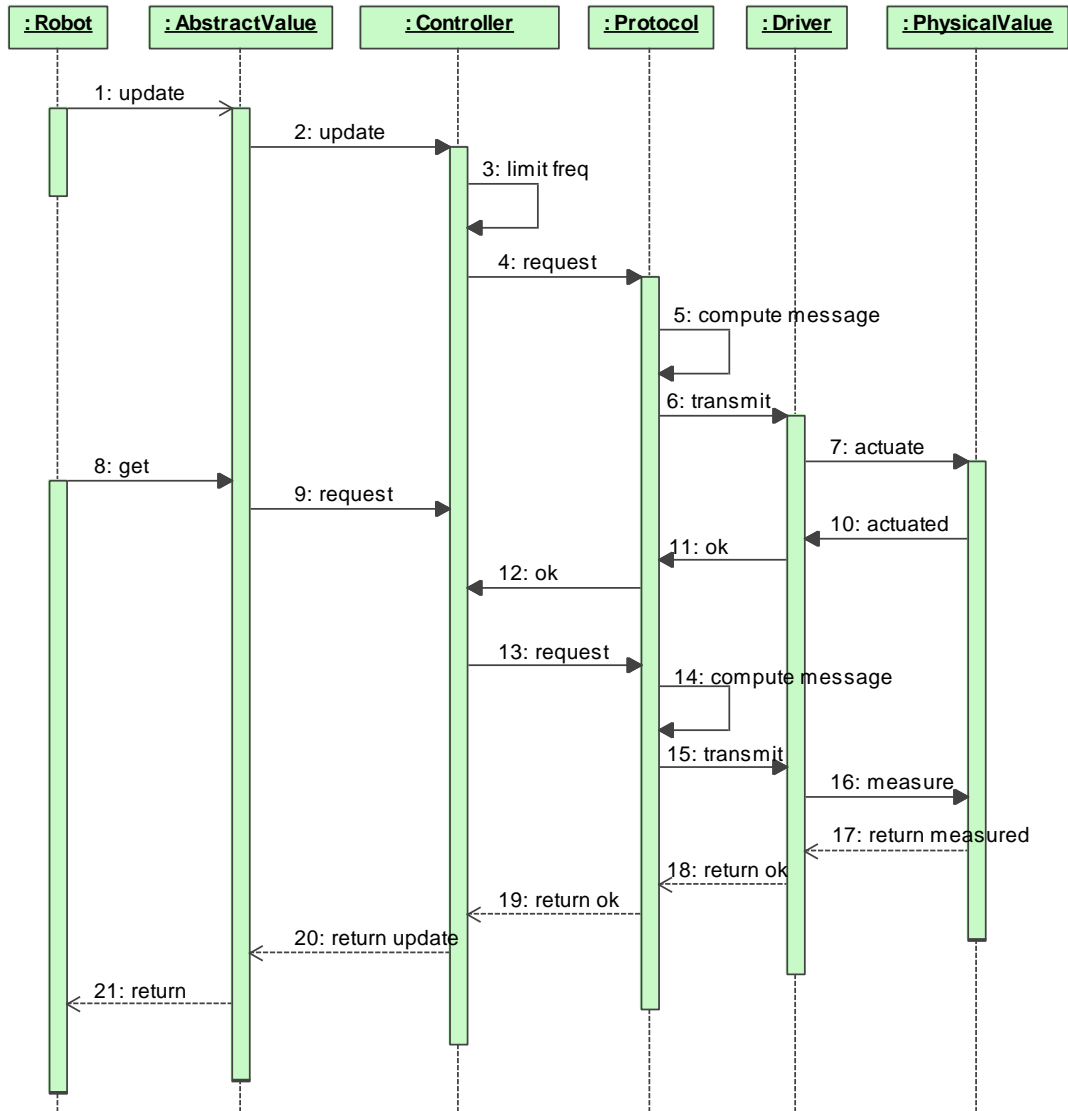


Figure A.2: Sequence diagram for protocol driver abstraction.

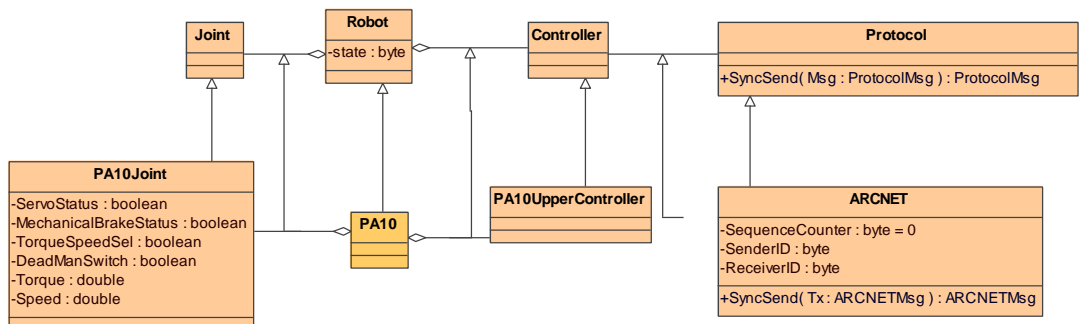


Figure A.3: Class diagram for ARCNET communication driver.

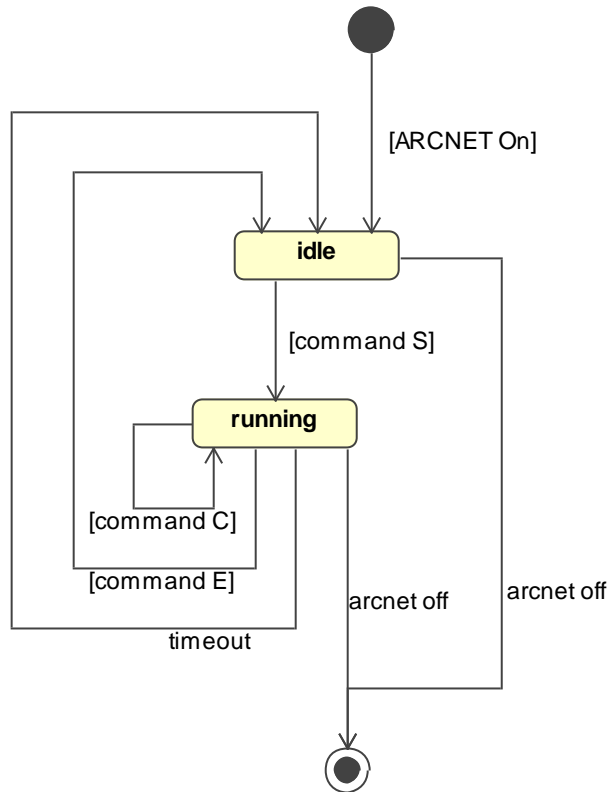


Figure A.4: ARCNET state diagram for MPA10.

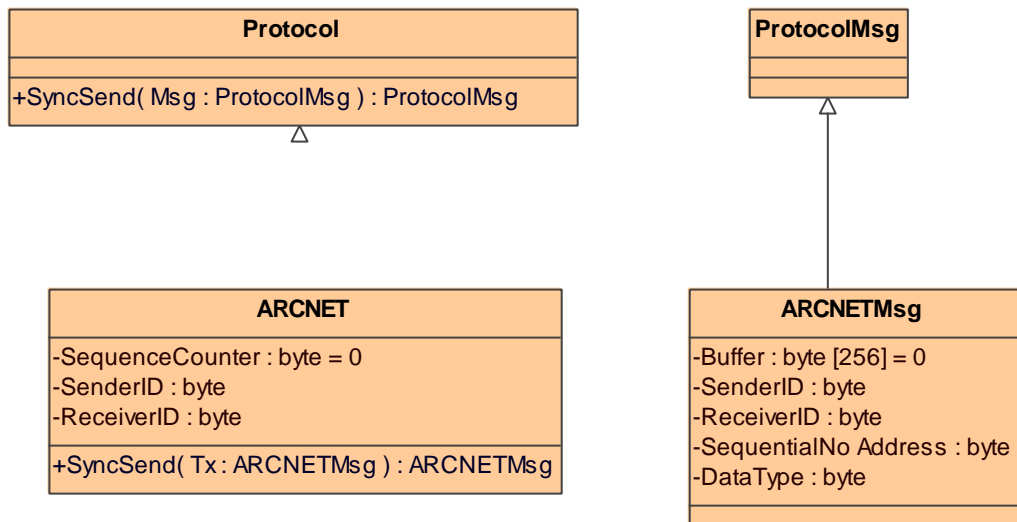


Figure A.5: Class diagram for concrete ARCNET protocol and message classes.

CURRICULUM VITAE

Aykut Kılıç was born in 25 may 1980. He has graduated from Ümraniye Anatolian Highschool in 1998. He began studying Electrical Engineering at Istanbul Technical University and got his BsC degree in 2002. He attended mechatronics engineering master degree programme and started working Ford Otosan as a software developer in 2002.